

ADOKETOCARPUS GEN. NOV., A MITRATE FROM THE LUDLOVIAN KILMORE SILTSTONE AND LOCHKOVIAN HUMEVALE FORMATION OF CENTRAL VICTORIA

MARCELLO RUTA AND PETER A. JELL

Ruta, M. & Jell, P.A. 1999 06 30: *Adoketocarpus* gen. nov., a mitrate from the Ludlovian Kilmore Siltstone and Lochkovian Humevale Formation of central Victoria. *Memoirs of the Queensland Museum* 43(1): 377-398. Brisbane. ISSN 0079-8835.

The mitrate *Adoketocarpus* gen nov. is the first representative of the Paranacystidae from Australia. It occurs in central Victoria with *A. acheronticus* sp. nov. in the Ludlovian Kilmore Siltstone and *A. janeae* sp. nov. in the Lochkovian part of the Humevale Formation. *Adoketocarpus* has a simplified plate arrangement on the convex surface and a strongly twisted orifice; plating of the plano-concave surface resembles that of Middle Ordovician *Enmitrocystella savilli* from Morocco suggesting that the paranacystids may derive from boreal mitrocystitids. Fewer lateral marginal plates of the plano-concave surface, loss and size reduction of distal plates and enlargement of proximalmost plates of the convex surface would attend evolutionary transition from boreal mitrocystitids to paranacystids. Paranacystids formed a clade whose origin and evolution were apparently in Gondwanaland, where they probably dispersed in the Ordovician/Silurian. □ *Paranacystidae, Adoketocarpus, Silurian, Devonian, Victoria.*

Marcello Ruta, Department of Palaeontology, Natural History Museum, Cromwell Road, London SW7 5BD, United Kingdom; Peter A. Jell, Queensland Museum, P.O. Box 3300, South Brisbane 4101, Australia; received 3 December 1997.

The known Australian carpodid fauna of 4 endemic genera with 6 species is more abundant than faunas from other parts of Gondwana. Some Australian carpodids have affinities with species from Europe and North America (Gill & Caster, 1960; Ruta, 1997a), whereas others have affinities with taxa from South America, South Africa and New Zealand (Caster, 1956, 1983; Caster & Gill, 1967; Philip, 1981; Haude, 1995; Ruta & Theron, 1997). The new genus described herein has its nearest relatives in the Lower Devonian of South America and South Africa.

Among Australian carpodids none are closely related to the new genus. *Rutrochypeus* is the only solute known from Australia; it occurs in the Lower Devonian of Kinglake, Victoria, with *R. junori* (Withers, 1933), *R. victoriae* Gill & Caster, 1960 and *R. ? withersi* Gill & Caster, 1960. The other 3 monotypic genera are mitrate stylophorans of the Anomalocystitida: *Tasmanicytidium burretti* Caster, 1983 from the upper Llandoverly Richea Shale of SW Tasmania, *Notocarpus garratti* Philip, 1981 from the upper Ludlovian part of the Humevale Formation near Whittlesea, central Victoria and *Victoriacystis wilkinsi* Gill & Caster, 1960 (Ruta, 1997a) from the lower Ludlovian in the Dargile Formation near Heathcote and the Melbourne Formation at Hawthorn.

Extensive collections of echinoderms from the mid-Palaeozoic of central Victoria made over many years, but mainly during the early 1980s, are housed in the Museum of Victoria. This paper deals with a new paranacystid mitrate genus from the Upper Silurian and Lower Devonian of central Victoria. It is important because: 1, it is the first Australian record for the Paranacystidae Caster, 1954; 2, its occurrence in the Upper Silurian is the earliest for the family, predating the Lower Devonian record in South America (Caster, 1954; Haude, 1995); 3, its anatomy can be reconstructed in detail, thus throwing light on several poorly known aspects of the paranacystids and prompting a new interpretation of their skeleton (Caster, 1954; Ruta, 1997c). 4, it provides additional evidence of the affinities between Siluro-Devonian mitrate faunas of Australia and the Malvinokaffric Realm (Caster, 1954, 1956, 1983; Gill & Caster, 1960; Caster & Gill, 1967; Philip, 1981; Parsley, 1991; Haude, 1995; Ruta & Theron, 1997; Ruta, 1997c).

LOCALITIES. The mitrates described in this work are from 4 different localities in the Museum of Victoria locality register (NMVPL) representing 3 horizons.

NMVPL252 Middendorp's Quarry at Kinglake West is marked on the map of Williams (1964) and discussed elsewhere (Ruta & Jell, 1999); it

occurs in the Humevale Formation and the brachiopod fauna indicates the *Boucotia janeae* Brachiopod Zone (Garratt, 1983) of mid Lochkovian age.

NMVPL1924 (=T95 of Williams (1964)) is in fine sandstones in the bed of Mathieson Creek, 2km S of the Kinglake West to Flowerdale Road. Carpoids are a minor component of an extensive fauna dominated by diverse crinoids and stelleroids and including brachiopods, bryozoans, corals (*Pleurodictyum* only), bivalves and several other minor groups. Williams (1964) showed this site to be in the same Sandstone Member (probably the Flowerdale Sandstone Member) as Collins Quarry near Kinglake West which is Lochkovian (Vandenberg, 1988) based on the brachiopods (Garratt, 1983).

NMVPL1927 is on the eastern bank of Broadhurst Creek, where it crosses the Kilmore to Wandong Road, SSW of Kilmore in central Victoria. The locality occurs at 37°20'30"S, 144°59'35"E (Grid Reference 220652) on the Kilmore 1:50,000 Geological Map (Vandenberg, 1992). The fossils come from the Kilmore Siltstone (Vandenberg, 1992), a sequence of predominantly thin (5-10cm), horizontally banded siltstones and very thin (less than 1cm), cross-bedded sandstones with rare, irregularly interbedded turbidite sandstones. The sequence is more than 3,500m thick. This huge thickness of siltstone indicates very rapid deposition on a tectonically stable shelf.

Graptolites indicate an early Ludlow age (Vandenberg, 1992) for the upper Kilmore Siltstone in the Kilmore district, from which most of the shelly faunas have been collected. Trilobites predominate, with rare brachiopods, bryozoans, ostracodes and rugose corals, all of which are concentrated mainly in coarse sandstones. Echinoderms are locally abundant in thick sandstone beds (Vandenberg, 1992). NMVPL 1927 occurs lower in the sequence and is most probably early Ludlow in age, although the possibility that it belongs to the late Wenlock cannot be ruled out.

NMVPL1960 refers to material excavated from a pipeline trench about 2km towards Kilmore along the Kilmore to Wandong Road from NMVPL1927 in similar lithology and horizon.

SYSTEMATIC PALAEOONTOLOGY

A standard anatomical nomenclature for mitrates does not exist (Caster, 1952; Caster & Gill, 1967; Ubaghs, 1967; Kolata & Jollie, 1982;

Jefferies, 1986; Cripps, 1990; Kolata et al., 1991; Parsley, 1991; Beisswenger, 1994; Ruta, 1997a, b; Ruta & Theron, 1997). The terminology of Ruta (in press) is followed for the external skeleton and plating pattern except that, for brevity, 'left' and 'right' replace 'anomalocystid' and 'abanomalocystid' respectively. For the internal anatomy, we use Ubaghs' (1967, 1969) nomenclature, although reference is necessary to some other sources (Jefferies, 1986; Jefferies, 1973; Jefferies & Lewis, 1978; Cripps, 1990; Beisswenger, 1994; Ruta & Theron, 1997).

Unless otherwise stated illustrations are of latex casts from decalcified siltstone, whitened with ammonium chloride sublimate.

Class STYLOPHORA Gill & Caster, 1960
Order MITRATA Jaekel, 1918
Suborder incertae sedis
Family PARANACYSTIDAE Caster, 1954

DIAGNOSIS (modified from Caster, 1954 and Ruta, 1997c). Plates A and C proximo-distally elongate, markedly different in shape and size; C separated from left DLM and left PLM by A. Left PM slightly larger than right PM, with chevron-shaped distal margin. Lateral and proximal marginal plates with well-developed subvertical projections. Skeletal sculpture of small elliptical knobs or tooth-like serrations along lateral margins of PLM plates, sometimes extending on proximal parts of lateral margins of left DLM and right EXM/ILM. Proximal 1/2-2/3 of convex body surface formed by proximo-distally elongate, shield-like C20 and C22. Distal part of convex surface of 2 smaller, subtrapezoidal plates with sinuous to gently concave lateral and distal margins and pronounced latero-distal angles. Small, subquadrangular to lozenge-shaped plate, possibly homologous with C21, between C20 and C22, proximally and subtrapezoidal plates, distally. Proximal part of appendage shorter than maximum width of each PM plate. Styloid with slightly expanded to flared, non-recumbent blades and proximal stout articulation process. Proximal ossicles of distal part of appendage expanded transversely and much more robust than successive ossicles.

Adoketocarpus gen. nov.

TYPE SPECIES. *Adoketocarpus acheromicus* sp. nov.

ETYMOLOGY. Greek *adoketos*, unexpected and *carpos*, a fruit; refers to body shape and unusual skeletal features. Masculine.

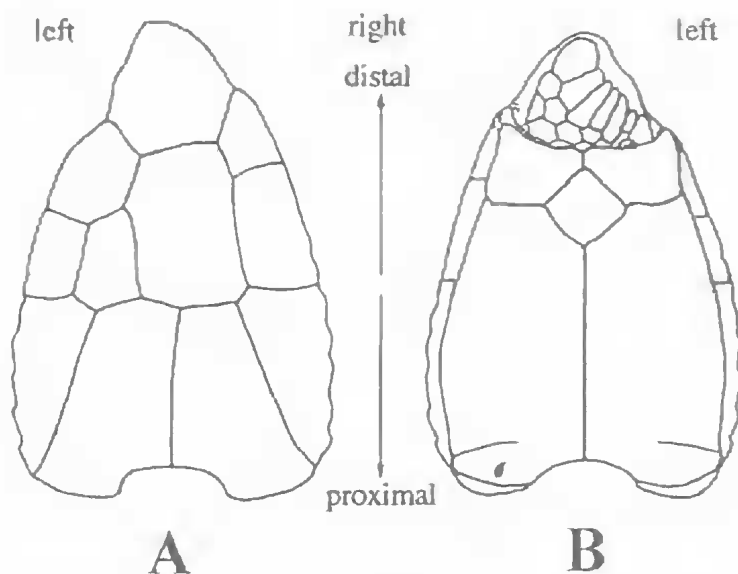


FIG. 1. Orientation of the skeleton of *Adoketocarpus acheronticus* gen. et sp. nov. A, plano-concave surface. B, convex surface.

DIAGNOSIS. C at least twice as wide as A. Length of left and right PLM exceeding that of other lateral marginal plates. Lateral serrations on PLM plates decreasing in size proximo-distally, sometimes extending on proximal part of lateral margins of left DLM and right EXM/ILM. Maximum width of proximal part of appendage less than maximum width of proximal margin of each PM plate.

***Adoketocarpus acheronticus* sp. nov.**
(Figs 1-2, 3D, 4-10, 11A,D,E, 12A-D)

ETYMOLOGY. Greek *Acheron*, a river of the underworld in Greek mythology; most specimens were collected on the bank of a stream.

MATERIAL. Holotype: NMVP100330. Paratypes: NMVP100331-100348 from NMVPL1927. Other material: NMVP100349-100356, QMF37202, 37208, 37212, 37213, 37214 from NMVPL1927; NMVPI49357-149358 from NMVPL1960.

DIAGNOSIS. Lateral body margins gently convex. Plate A subpentagonal to wedge-shaped, slightly to much wider proximally than distally and c. 1/2 as large as C. Right LOP slightly smaller than C, roofing over the body orifice, with almost straight proximo-lateral margins and sinuous latero-distal margins; distal process pronounced, with blunt, rounded end. Left DLM much shorter than right EXM/ILM, about as long as and slightly narrower than left LOP. Left LOP

larger than right DLM, contributing to distal 1/3 of left lateral body margin. Subvertical projections of left and right PM straight to gently convex externally; suture between left and right PM bending slightly rightward distally. Plate C about as wide proximally as distally, with chevron-shaped proximal margin. Suture between A and C sinuous, gently concave rightward proximally, more deeply concave leftward distally. Suture between distal subtrapezoidal plates of convex surface shorter than their proximal and proximo-medial margins.

DESCRIPTION.
EXTERNAL. Body longer than wide, ovato-lanceolate to

pyriform, slightly (Figs 1-2, 3D, 4A-E, 5C, 11A,B,D). Maximum width about twice as far away from distal process of right LOP as from proximal excavation for appendage insertion. Lateral margins more strongly convex proximally than distally; right margin slightly longer than left margin. Subvertical projections of lateral marginal plates visible when the convex surface is oriented towards the observer (Figs 4F, 6A,C,D, 7A,B, 11E, 12D). Distal body orifice twisted leftward and framed by radially arranged platelets of different shape and size (Figs 4F, 6A-D). Plano-concave surface slightly raised along lateral margins and near proximo-lateral angles and shallower centrally (Figs 4A-E, 5A-D). Maximum curvature of convex surface at the level of its proximal 1/3 (Figs 6A, C, 7B, 9B).

Measurements. Holotype (Fig. 4A): c.4.7mm wide and 6.7mm long. Smallest specimen (Fig. 4C,F): c.2.7mm wide and 3.7mm long. Largest specimen (Fig. 4E): estimated body width and length c.5.7mm and 7.7mm, respectively.

Plano-concave surface. Weakly concave surface of 11 medium to large plates. Marginal plates in 2 groups of 3, a distal element roofing over the body orifice and 2 proximal elements contributing to excavation for appendage insertion (Figs 1A, 2A, 3D, 4A-E, 5A,C, 11A,B,D). Height of subvertical projections of lateral marginal plates approximately constant over most of their length,

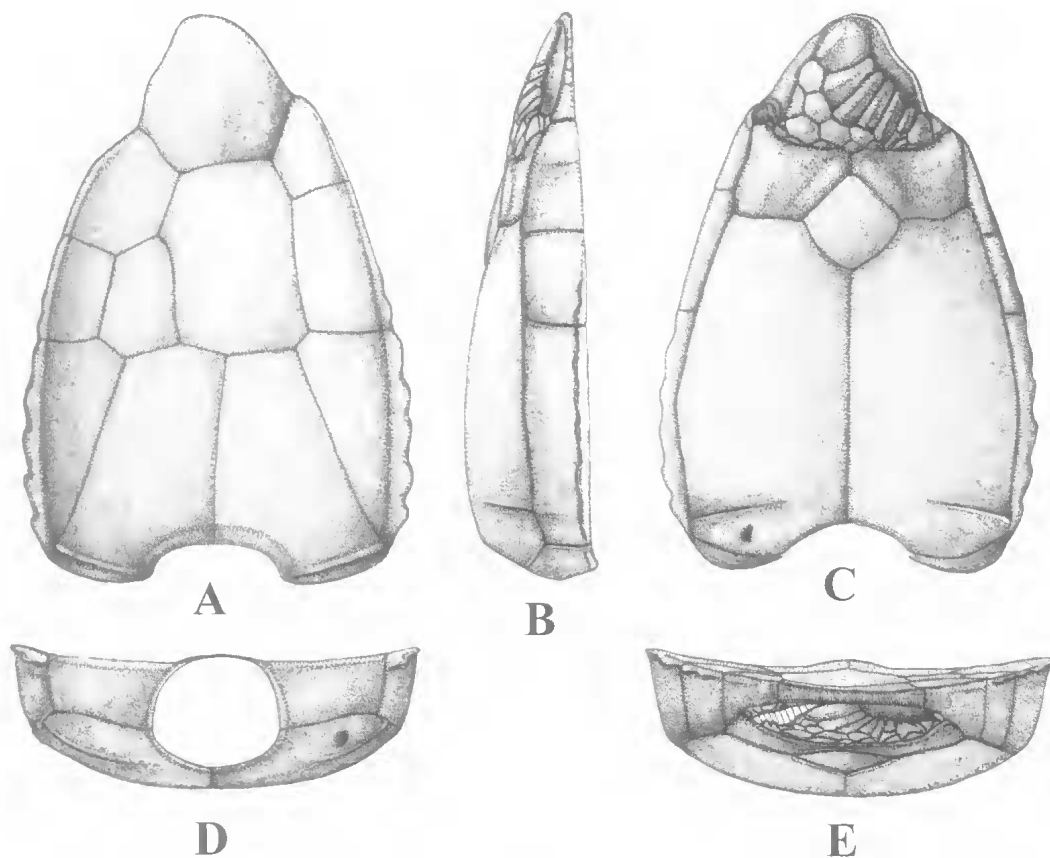


FIG 2. Reconstruction of *Adoketocarpus acheronticus* gen. et sp. nov. (appendage omitted). A, plano-concave surface, B, left lateral view. C, convex surface. D, proximal view. E, distal view (hatched area shows space possibly occupied in life by polygonal plates).

only slightly decreasing near latero-distal angles of plano-concave surface and at the level of proximal 1/3 of both left and right PLM (Figs 2B, 4D-E, 5A,C, 6A,C, 7A, 11E); subvertical projections of PM plates higher than those of lateral marginal plates, rectangular to trapezoidal in proximal view and flat to gently convex externally (Figs 2A-D, 4D, 5A-D). Subpentagonal left LOP and trapezoidal right DLM forming latero-distal angles of plano-concave surface: left LOP slightly wider and longer than right DLM. Left DLM and right EXM/ILM subrectangular and proximo-distally elongate; length of left DLM e. 2/3 that of right EXM/ILM. Left and right PLM subequal in shape and size, triangular and contributing to proximo-lateral angles of body; lateral margins of both plates PLM with 4-5 serrations rapidly decreasing in size proximo-distally and either gradually merging into each other or neatly separated; 2-3 proximalmost

serrations with blunt, rounded apex, steep distal margin and gentle proximal margin; 1-2 very shallow serrations near proximal 1/3 of lateral margins of left DLM and right EXM/ILM (Figs 1A, 2A, 3D, 4A-D, 5C, 7A, 11A). Distal margin of left PM longer than distal margin of right PM and chevron-shaped, the right arm of the chevron being as long as or longer than its left arm; median 1/2 of proximal margins of both plates PM excavated for insertion of appendage; suture between such plates generally bending slightly rightward distally; transverse thickening sometimes observed along their proximal margins (Figs 4D-E, 5A-D). Irregularly pentagonal right LOP slightly smaller than C, with prominent plectrum-shaped to semicircular distal process, gently sinuous latero-distal margins and almost straight proximo-lateral margins (Figs 4A-E, 5A,C, 11A,B,D); distal process immediately left of longitudinal body axis. Plate A

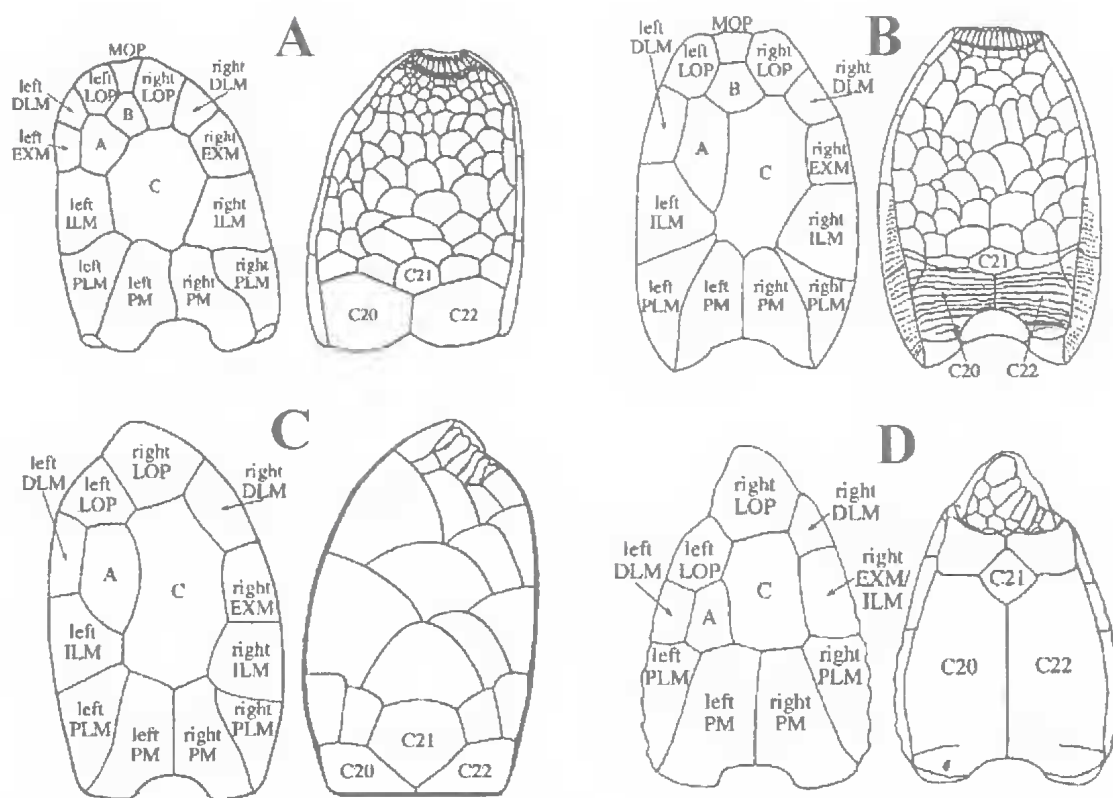


FIG. 3. Plate nomenclature of the plano-concave (left) and convex (right) surfaces in 3 mitrocystitids and in *Adoketocarpus acheronticus* gen. et sp. nov. Specimens not to the same scale. A, *Mitrocystella barrandei* (redrawn from Ubaghs, 1968). B, *Mitrocystella incipiens* (simplified from Jefferies, 1986). C, *Eumitrocystella savilli* (modified from Beisswenger, 1994). D, *Adoketocarpus acheronticus* gen. et sp. nov.

subpentagonal to wedge-shaped, longer than wide, slightly to much wider proximally than distally, comparable in size with left and right DLM (Figs 4A-D, 5C, 11A,B,D) and in contact with left LOP latero-distally, left DLM laterally, left PLM proximo-laterally and left PM proximo-medially. C twice as long and wide as A and in contact with right LOP distally, right DLM latero-distally, right EXM/ILM laterally, right PLM proximo-laterally and right and left PM proximally (Figs 2A, 3D). Suture between A and C with deep leftward concavity distally and less pronounced rightward concavity proximally (Figs 4A-D).

Convex surface. Convex surface of 5 small to large plates symmetrically arranged in centre, plus 8 plates extending up lateral and proximal margins from plano-concave surface. Proximal 2/3 of convex surface of large, proximo-distally elongate, shield-like C20 and C22 plates, 1.5-2 times longer than wide (Figs 1B, 2C, 3D, 4F, 6A,C, 7B, 9A-C, 12B,D). Lateral 1/2 of proximal

margins of such plates straight to strongly convex; median 1/2 deeply excavated for appendage insertion; lateral margins of both plates gently to moderately convex, sometimes showing abrupt curvature about half-way along their length; lateral and proximal margins merging into each other smoothly or at c.120° (Figs 4F, 6A,C-D, 7B,8B-D, 9A-C, 11C,E). Proximo-lateral part of external surface of both C20 and C22 distinctly sloping, almost vertical with respect to the rest of the plate in its distal 1/2 and delimited distally by straight, slightly pronounced keel with steeper distal and gentler proximal slope (Figs 2B-D, 6C, 7B, 9B-C). Keels running latero-medially and proximo-distally from proximo-lateral angles of both C20 and C22, their length being less than 1/2 the width of these plates. External margin of small facet for articulation with plates PLM visible on both C20 and C22 just latero-distal to lateral end of each keel (Figs 1B, 2B-D, 4F, 6A, C, 7B, 9B). Sub-elliptical to teardrop-shaped pit proximal to

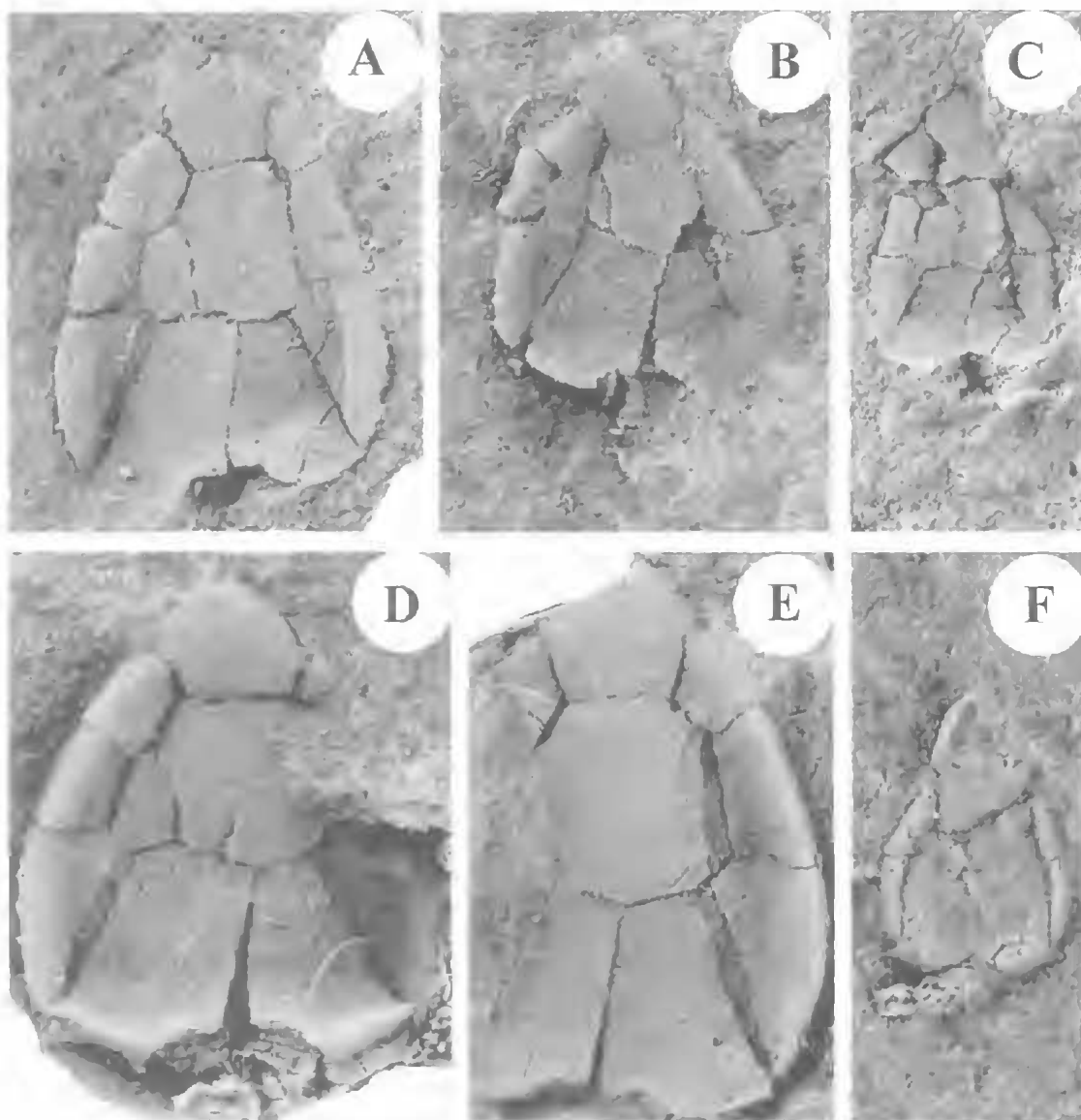


FIG. 4. *Adoketocarpus acheronticus* gen. et sp. nov., all from NMVPL1927, $\times 10$. A-E, plano-concave surface, F, convex surface. B, D, F, showing part of the appendage. A, NMVPL100330, holotype. B, NMVPL100331. C, E, NMVPL100332. D, NMVPL100333. E, NMVPL100334.

median 1/3 of keel on C20 (Figs 1B, 2B-D, 6C, 7B, 9B). Distal 1/3 of convex surface occupied by 2 subtrapezoidal plates, slightly wider than long and in contact with each other along very short, straight suture and with C20 and C22 along gently sinuous sutures; latero-distal angles of subtrapezoidal plates with distally directed, blunt-ended processes (Figs 1B, 2B-C, E, 3D, 4F, 6A-D, 9B). Subquadrangular to lozenge-shaped C21 with straight to slightly convex margins in

contact with medio-distal margins of C20 and C22 and with medio-proximal margins of subtrapezoidal plates (Figs 2B-C, E, 6A-D, 7B, 9B).

Distal orifice. Body orifice strongly twisted leftward, roofed over by right LOP and floored by 6-7 platelets arranged radially (Figs 1B, 2B-C, E, 4F, 6A-D). Right platelet subelliptical, with major axis almost perpendicular to longitudinal body axis; remaining platelets subrectangular to spike-shaped and decreasing progressively in

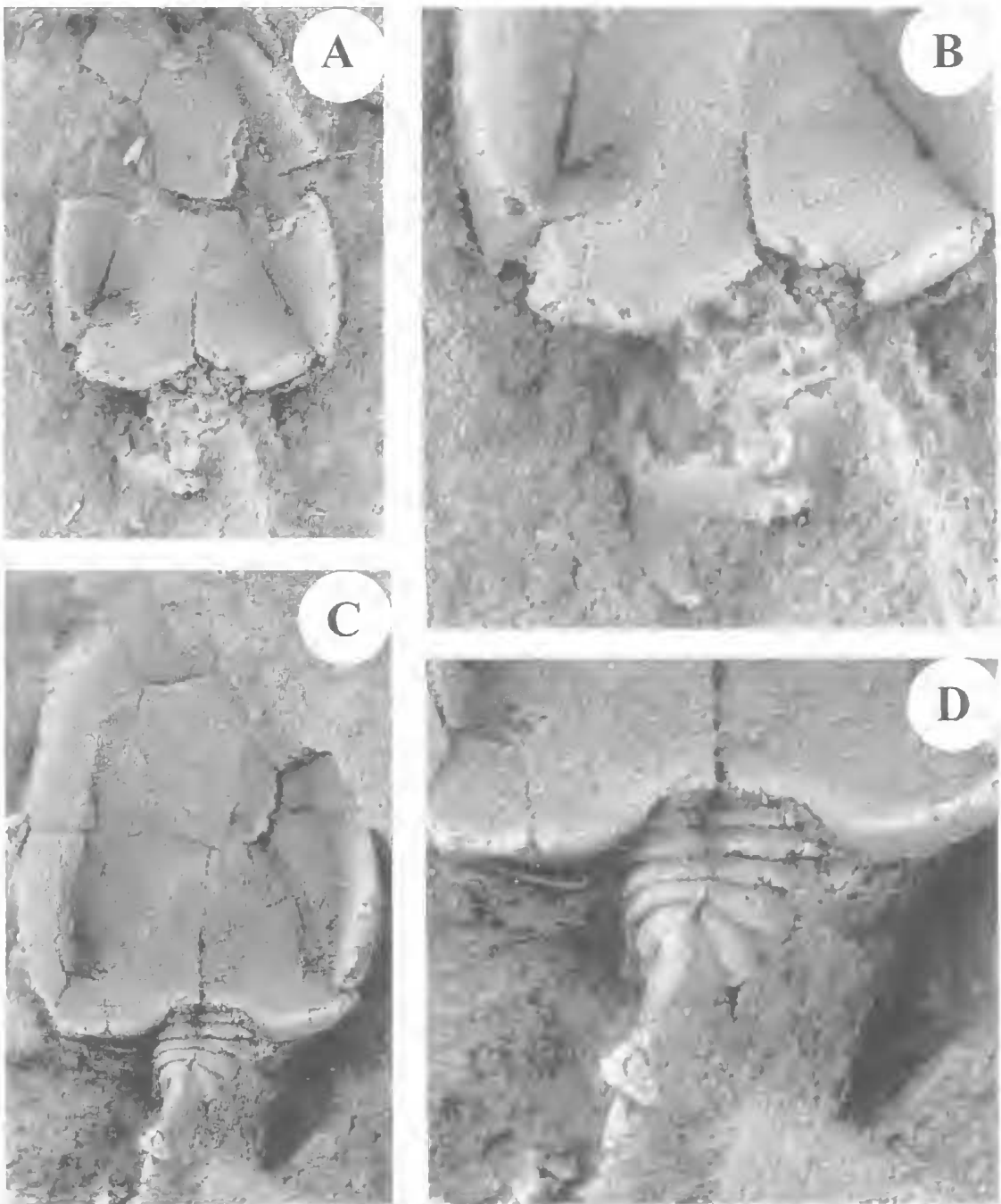


FIG. 5. *Adoketocarpus acheronticus* gen. et sp. nov., all from NMVPL.1927. A,C, plano-concave surface. B,D, proximal part of appendage and styloid. A,B, NMVP100335, $\times 10$ and $\times 20$, respectively. C,D, NMVP100336, $\times 10$ and $\times 20$, respectively.

size from right to left: left platelet subtriangular, with major axis parallel to longitudinal body axis. Polygonal elements of irregular shape inserted

between proximal margins of orifice platelets and distal margins of subtrapezoidal plates. more numerous on the right than on the left, smaller

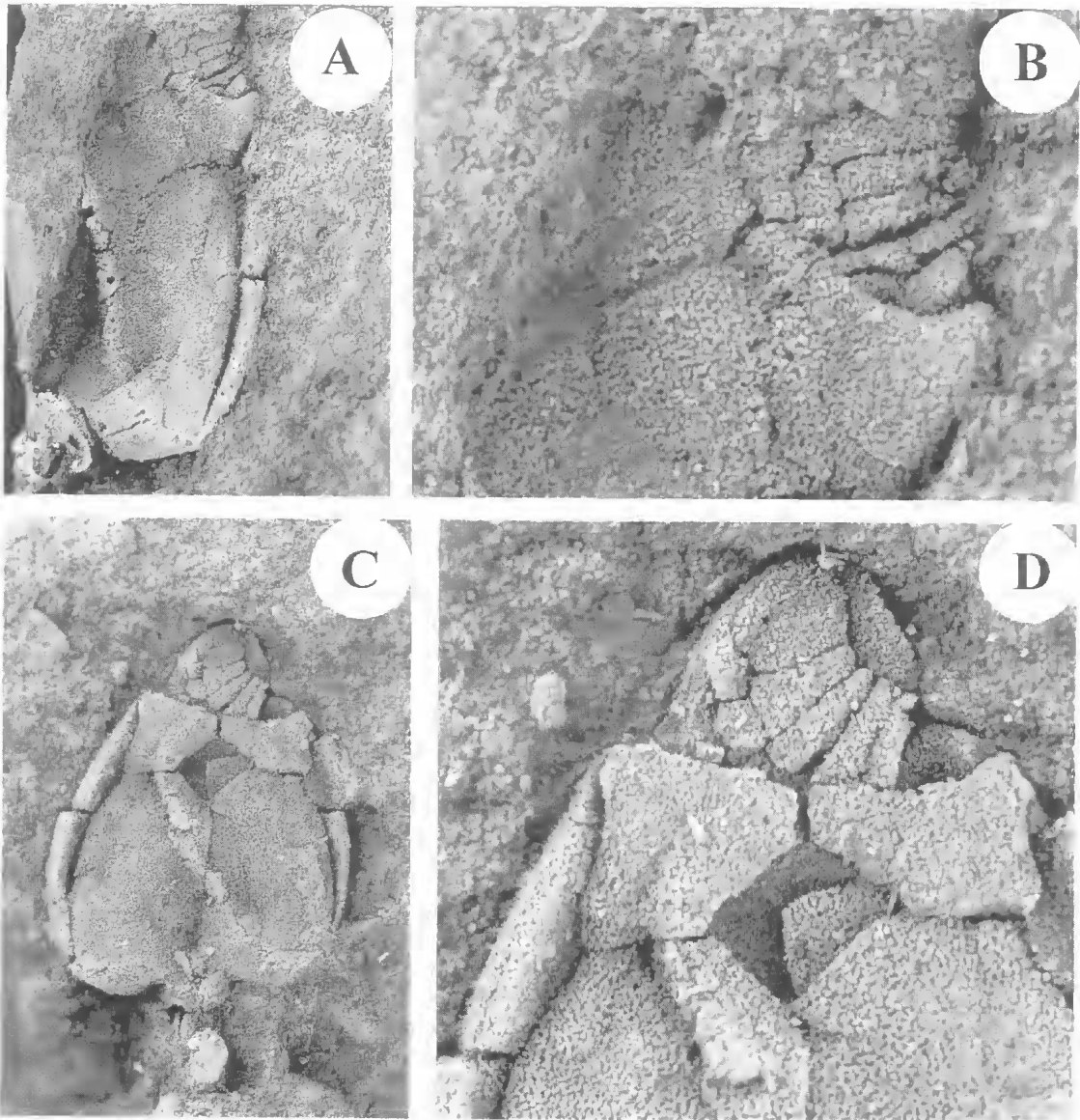


FIG. 6. *Adoketocarpus acheronticus* gen. et sp. nov., all from NMVPL 1927. A, C, convex surface and proximal part of appendage. B, D, close-ups of orifice platelets. A, B, NMVPL100337, $\times 10$ and $\times 30$, respectively. C, D, NMVPL100338, $\times 10$ and $\times 25$, respectively.

and transversely elongate near distal margins of subtrapezoidal plates, larger near proximal margins of orifice platelets; polygonal elements probably also covering proximal part of right latero-distal margin of right LOP (Fig. 6C-D).

Stereom. Plates of plano-concave surface with irregular, highly variable external texture, mainly consisting of subcircular to subelliptical pores separated by trabeculae (Figs 4A-E, 5A-C).

Thinner trabeculae and smaller subcircular pores visible near lateral body margins. Trabeculae often forming a fringe near plate sutures, where the pores are narrow and elongate and arranged radially. Irregularly radiating pattern of sinuous, elongate, bifurcating trabeculae on marginal and subcentral plates, especially near their centres; adjacent trabeculae often sending at irregular intervals shorter, transverse trabeculae delimiting subrectangular to subelliptical pores.

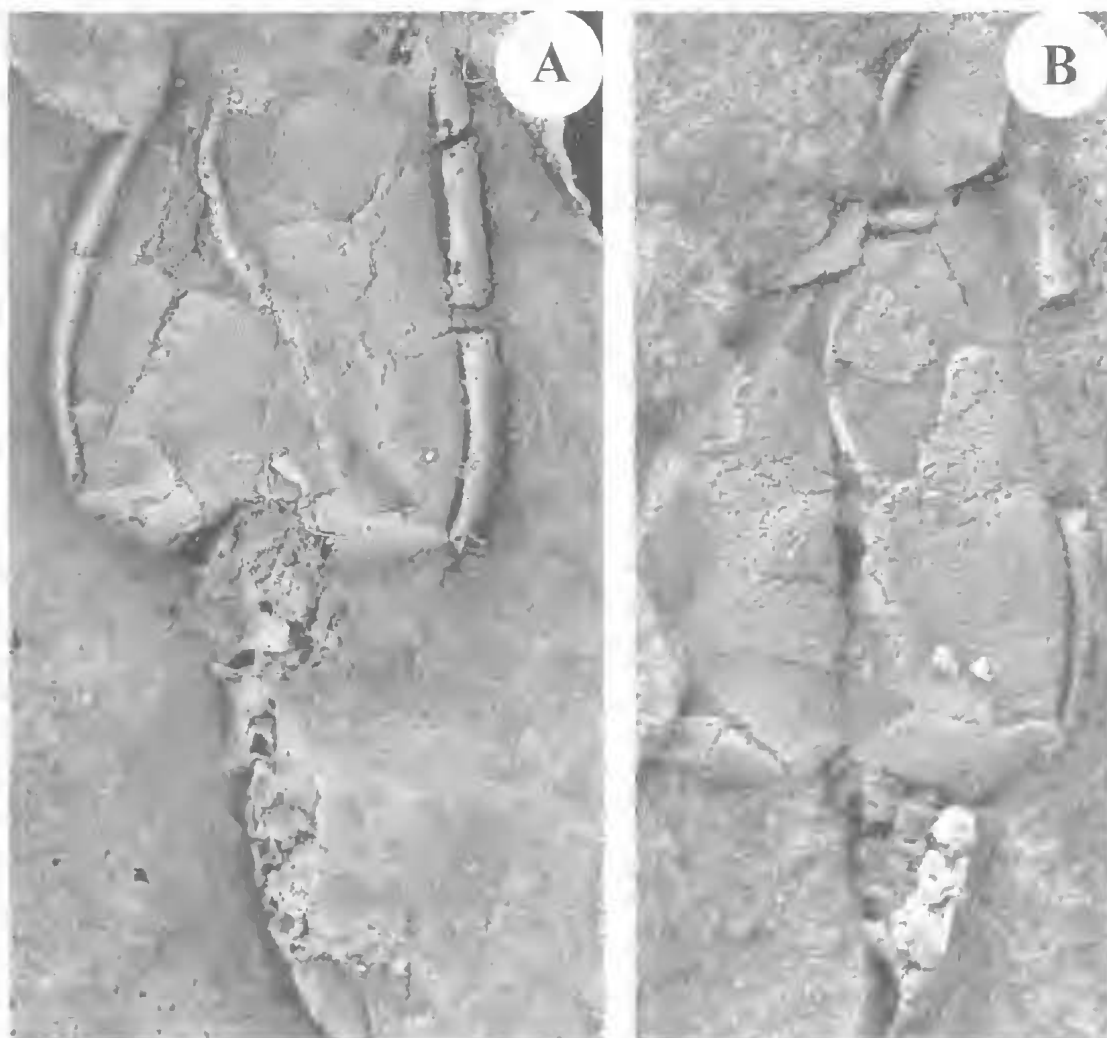


FIG. 7. *Adoketocarpus acheronticus* gen. et sp. nov., all from NMVPL1927. A, NMVP100339, inside of plano-concave surface and partially preserved appendage, $\times 10$. B, NMVP100340, partially preserved convex surface, distal 1/3 of inside of plano-concave surface and disrupted appendage, $\times 15$.

Stereom of subvertical projections of lateral marginal plates generally compact or consisting of minute subcircular pores. Stereom of convex surface almost uniformly composed of circular pores and short trabeculae, the latter arranged radially near the plate sutures (Figs 4F, 6A-D, 7B, 9B-C). Stereom of orifice platelets coarsely granular or with very shallow pits surrounded by weak ridges (Figs 4F, 6B,D).

INTERNAL. Plate C, right LOP (in part) and left and right PM reveal most of the inside of the plano-concave surface, but little is known about the interior of the lateral marginal elements (Figs 7A, 9B-C). So far as the convex surface is

concerned, only the internal aspect of C20 and C22 is known in detail, whereas the inside of the distal 1/3 of this surface is only partially preserved.

Plano-concave surface. Right latero-distal angle of internal surface of right LOP occupied by median 1/3 of subcircular depression straddling suture with right DLM and continuing on adjacent part of internal surface of latero-distal angle of this plate (Figs 1B, 2C, E, 6C-D). Internal side of plano-concave surface divided into 2 fields by oblique septum (Ubaghs, 1967) (= oblique ridge of Jefferies, 1986) (Figs 7A-B, 8A; see in Fig. 10B); distal 1/3 of septum with marked

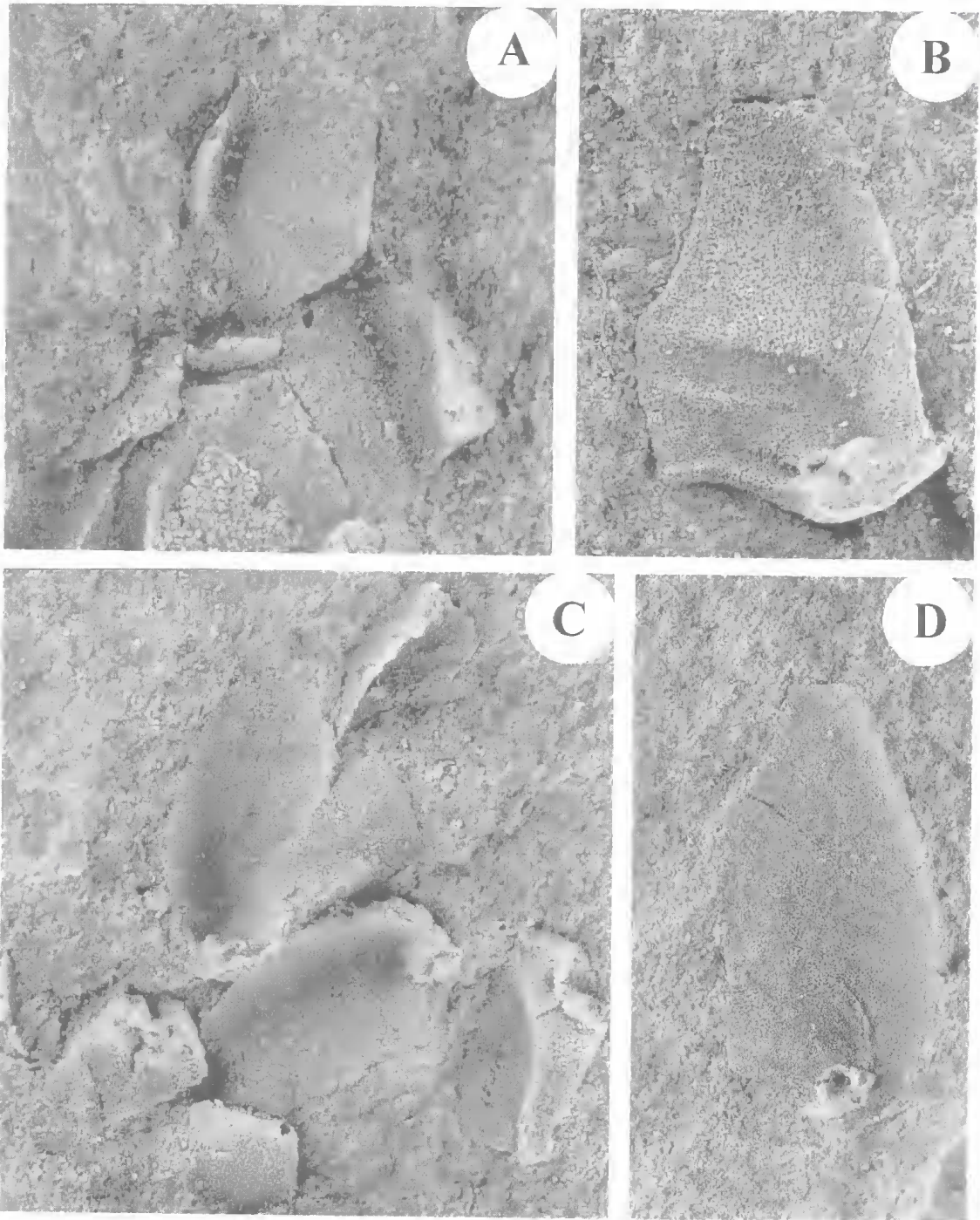


FIG. 8. *Adoketocarpus acheronticus* gen. et sp. nov., all from NMVPL1927. Internals of skeletal plates. A, NMVP100340, disrupted distal 1/3 of plano-concave surface; the element near top centre is right LOP, $\times 25$. B, NMVP100342, inside of C20, $\times 20$. C, NMVP100343, plates C20, C21, C22, left and right PM, left PLM, $\times 16$. D, NMVP100344, inside of C20, $\times 12$.

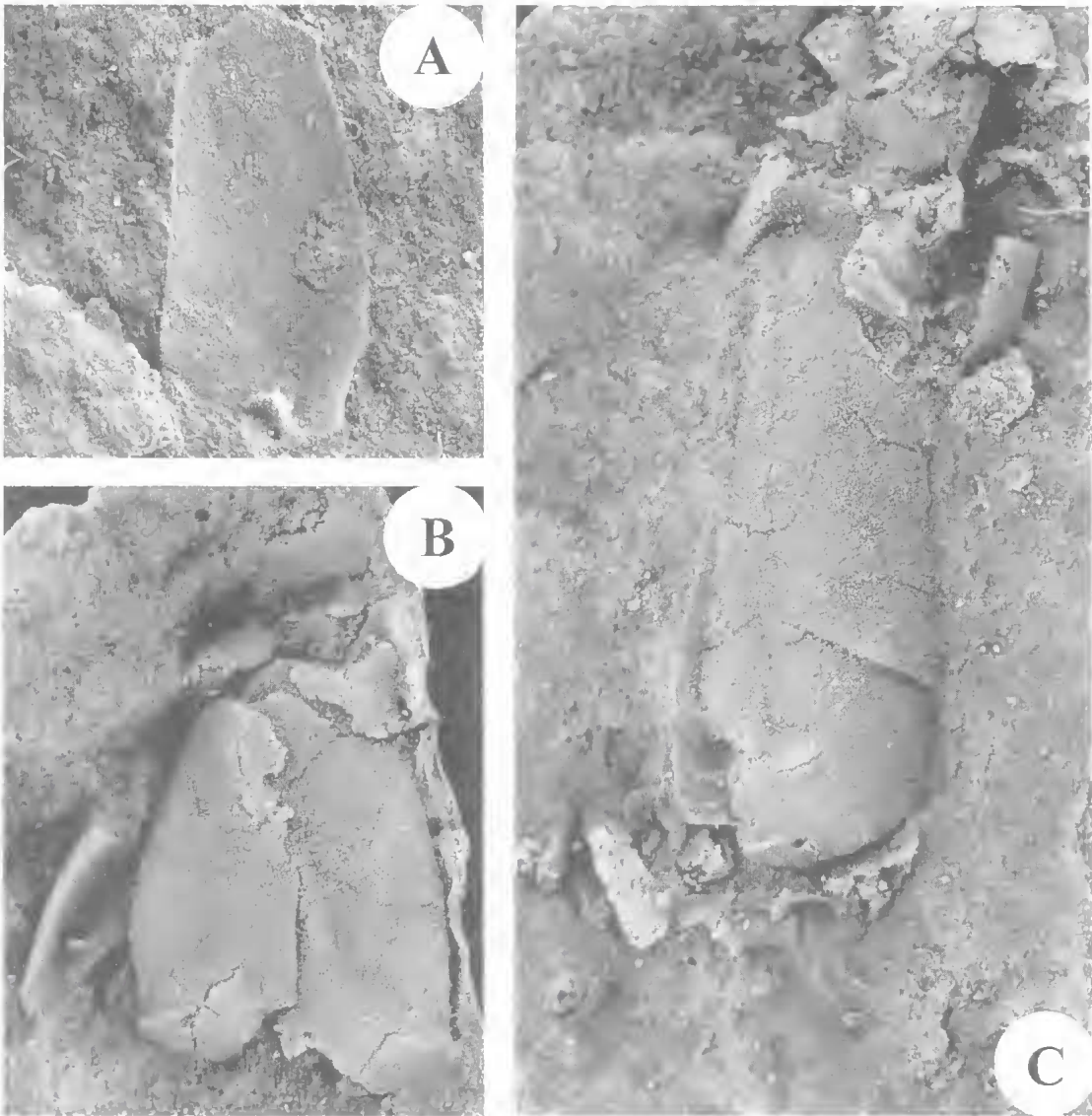


FIG. 9. *Adoketocarpus acheronticus* gen. et sp. nov., all from NMVPL1927. A, NMVPL100345, inside of C20, $\times 12$. B, NMVPL100346, convex surface, partially disrupted distal 1/3, $\times 10$. C, NMVPL100347, slightly damaged C20 in external view, $\times 12$.

rightward convexity occupying distal 2/3 of internal surface of C (Figs 6C-D, 7A-B, 8A); distalmost end rapidly weakening where it straddles suture between C and right LOP and vanishing distally on the internal surface of the latter: proximal 2/3 of septum straight, thicker than convex part and bending slightly to the right in cross-section: convex part passing gradually into straight part: boundary between these 2 parts delimited by elongate and poorly defined thickening (= diminutive spur of Ubaghs, 1967

and base of middorsal process of Jefferies, 1986) (Fig. 7A-B): straight part of septum running obliquely from internal side of proximal 1/3 of C to internal side of left PM, straddling suture just lateral to medio-distal angle of left PM (Fig. 10A-B).

Proximalmost end of septum merging into cup-like left scutula (Ubaghs, 1967) (= dorsal calcitic cup of left pyriform body of Jefferies, 1986) (see in Fig. 10B) delimited by slightly raised, thick, subcircular scutular rim. Deep transverse furrow

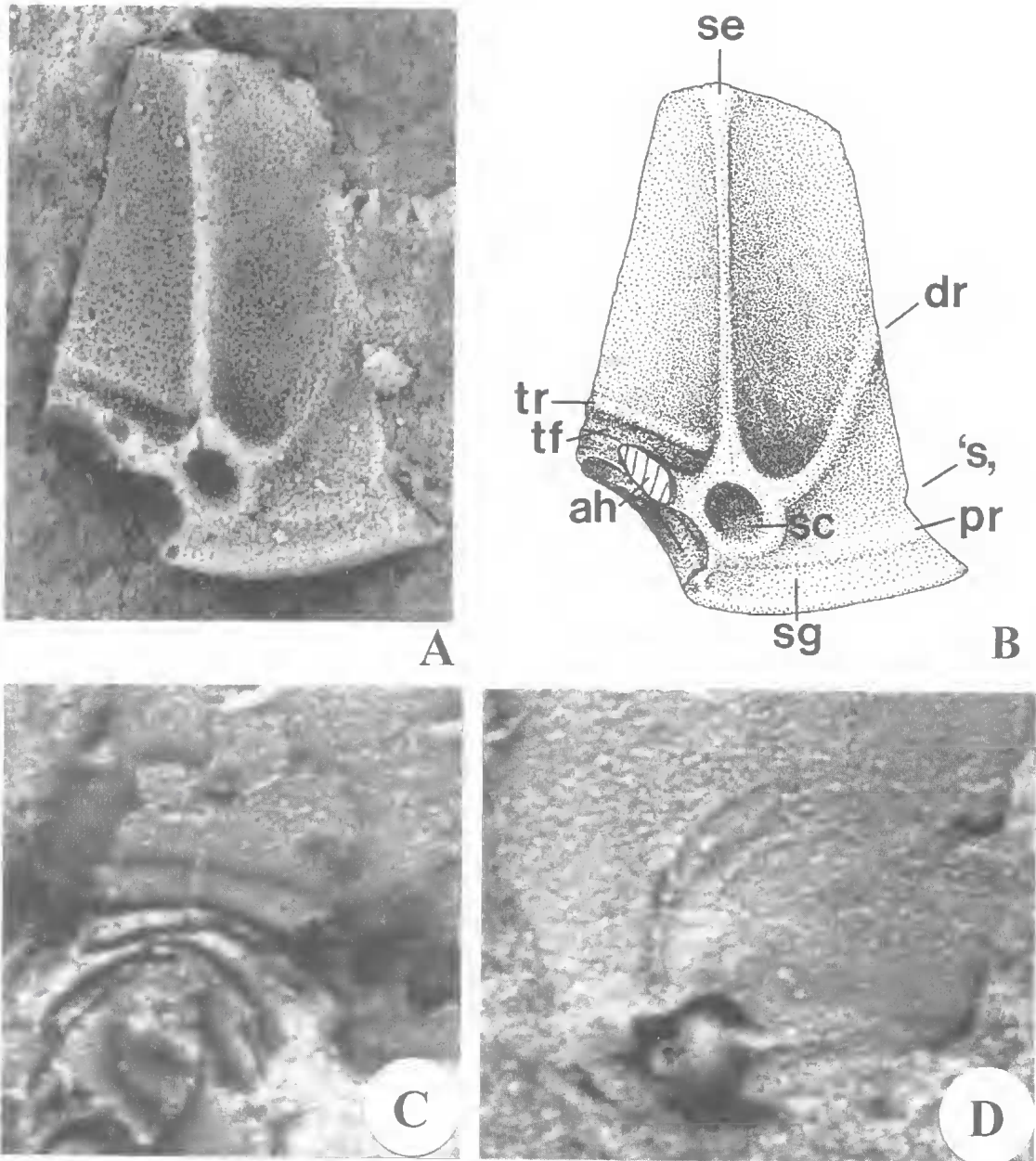


FIG. 10. *Adoketocarpus acheronticus* gen. et sp. nov., from NMVPL1927, internal surface of left PM plate. A. NMVP100348, $\times 25$, latex cast coated with ammonium chloride. B, camera lucida drawing of the same specimen; abbreviations as in text. C, NMVP100339, natural internal mould of proximal 1/3 of the 2 PM plates, $\times 25$. D, NMVP100344, natural internal mould of proximal 1/3 of C20, $\times 25$.

(= transverse anterior groove of Ubaghs, 1967 and anterior boundary of posterior eocloom of Jefferies, 1986) (tf in Fig. 10B) running from medio-distal part of seutular rim to median margin of both left and right PM and delimited distally by prominent transverse ridge, straight to

slightly convex distally (tr in Fig. 10B). On the left PM, the median end of such a ridge merges into the proximalmost end of the septum, where the latter becomes confluent with the medio-distal part of the seutular rim. Two slightly curved ridges on internal side of the left PM plate.

poorly developed or absent on the right PM, running almost parallel to each other or strongly diverging medio-laterally, and less robust than proximal part of septum; distal ridge (dr in Fig. 10B) projecting proximo-distally or transversely along gently curved direction from lateral wall of scutular rim to lateral margin of both PM plates where it widens and becomes less pronounced; distal ridge of left PM probably corresponding to accessory septum of Ubaghs (1967) (= posterior boundary of left pharynx of Jefferies, 1986); proximal ridge (pr in Fig. 10B) slightly shorter than distal ridge, almost straight and parallel to proximal margin of each of the two PM plates. Right PM differing from left PM in the small pit (= infundibulum of Ubaghs, 1967 and pit for dorsal end of lateral line ganglion of Jefferies, 1986) lying proximo-lateral to right scutula (Fig. 8C). Shallow groove (sg in Fig. 10B) for articulation with C20 and C22 running parallel to lateral part of proximal margins of left and right PM, and becoming progressively shallower near its lateral end; median end of groove interrupted by small ridge projecting latero-medially from medio-proximal part of scutular rim to lateral angle of external margin of excavation for appendage articulation (= cerebral basin of Jefferies, 1986). Proximalmost part of internal side of lateral margin of left and right PM showing 'step' ('s' in Fig. 10B) delimiting sudden change in the curvature of this margin and presumably representing interlocking articulation with left and right PLM respectively. Median part of both left and right scutular rim merging medially into transversely expanded area occupying median 1/3 of internal margin of excavation for appendage articulation, and presumably representing basal portion of each of the 2 apophyseal horns (Ubaghs, 1967) (=hypocerebral processes of Jefferies, 1986) (ah in Fig. 10B), not preserved in available material. Excavation on both PM plates consisting of shallower distal and deeper proximal parts; distal part (=prosencephalar part of cerebral basin of Jefferies, 1986) delimited by internal margin of excavation and by thin ridge running along slightly oblique direction from bases of apophyseal horns to proximo-medial angle of both plates; distal part (=deuterencephalar part of cerebral basin of Jefferies, 1986) delimited by above mentioned thin ridge and by external margin of excavation.

Convex surface. Cup-like co-operculum (Ubaghs, 1967) (= dorsal calcitic cup of pyriform body of Jefferies, 1986) near proximo-lateral angles of C20 and C22 (Figs 8B-D, 9A),

delimited by rim with thicker proximo-lateral and thinner medio-distal margins; rim interrupted medially by short, deep, transverse sulcus extending from excavation of co-operculum to portion of inner surface between co-operculum and proximal margins of C20 and C22; at the level of sulcus, both ends of co-opercular rim continue medially into slightly raised ridges parallel to median excavation of proximal margin of C20 and C22, gently convex distally and delimiting very shallow groove. Lateral wall of left and right co-opercula merging gradually into proximalmost part of lateral margin of both C20 and C22. Lateral 1/2 of proximal 1/3 of internal surface of both plates much deeper than the rest of the internal surface and showing 2 ridges (= ? n1 and n3 branches of palmar complex of Jefferies, 1986) projecting from distal wall of co-operculum, running close to each other distally for a short distance, then bending slightly medially and diverging from each other before disappearing abruptly medially (Figs 8C-D, 9A). Proximo-lateral part of co-opercular rim of C20 (Figs 8B, D, 9A) housing small subcircular pit (= pit of lateral line ganglion of Jefferies, 1986), c. 1/3 size of co-operculum and corresponding in position to infundibulum on inner surface of right PM. Straight, poorly pronounced ridge (= ? ventral anterior boundary of posterior coelom of Jefferies, 1986) running obliquely from a point just distal to each co-operculum to median margin of C20 and C22, at c.45° to longitudinal body axis (Fig. 8D). Transversely elongate facet for articulation with PM plate visible along lateral 1/2 of distal margins of C20 and C22, immediately proximo-lateral to co-opercula.

Stereom. Internal texture of subcentral and lateral marginal elements of plano-concave surface resembling external texture in the radial arrangement of trabeculae and pores (Figs 7A-B, 8A). Stereom of inside of left and right PM (Figs 8C, 10A) consisting of irregular meshwork of stout trabeculae and extremely irregular pores of different shapes and sizes, replaced by more compact texture on septum, scutular rim and bases of apophyseal horns as well as along proximal edge of both PM plates. Elongate, sometimes confluent pores along proximal and distal ridge on lateral half of PM plates. Stereom of excavation for appendage insertion with generally small, rounded pores and thin trabeculae (Figs 8B, D, 9A, 10A). Texture of inside of C20 and C22 consisting of regularly arranged circular pores, slightly smaller peripherally than

centrally. Stereom of co-opercula compact (Figs 8B-D, 9A).

APPENDAGE. *Proximal part.* 5-6 tetramerous rings overlapping each other proximo-distally; degree of overlap greater proximally than distally; distalmost ring slightly smaller than others and tightly wrapped around proximal styloid process; latero-distal angles of ring plates gently rounded (Figs 2A-B, 4B, D, F, 5A-D, 6A, C).

Intermediate part. Styloid with robust, stout proximal blade, triangular in section, less expanded transversely than distal blade and carrying a blunt apex; distal blade slightly bent towards the proximal blade in lateral view and with small, flat, triangular distal bearing surface. Sharp longitudinal keel running between the two blades, with parabolic outline in lateral view. Lateral styloid surfaces gently concave (Figs 5A-D, 12C).

Distal part. Few proximal ossicles preserved (mostly disarticulated), subrectangular in lateral view and apparently poorly developed, blunt apices, except in the first two ossicles, possibly carrying a small distal bearing surface (Figs 7A,B, 12A-D).

Stereom. Minute pores and thin trabeculae centrally on proximal ring plates and styloid; more compact stereom near margins of ring plates and on ossicles.

REMARKS. *Adoketocarpus acheronticus* displays little morphological or ontogenetic variation, as evidenced by small changes in the shape and proportions of several isolated skeletal elements of different sizes, which presumably belong to individuals of different ages, and by the similar proportions of complete specimens. The largest known individuals are either pyriform or ovato-lanceolate, whereas small to medium-sized individuals are only slightly longer than wide and their lateral margins are convex. Such differences are only partly caused by deformation. Deformation is, however, negligible in most cases, as the specimens are often found slightly disrupted but without signs of breakage. Likewise, disarticulated plates lying in proximity to each other are rarely broken; often, they are turned upside down or slightly rotated.

The right LOP, A, left and right PLM, left and right PM and C20 and C22 plates are most variable. The right LOP is sutured to the rest of the skeleton in most specimens, slightly displaced in a few specimens and rarely isolated. In the smallest specimen (Fig. 4C,F), the right

LOP is more asymmetrical and elongate proximo-distally than in larger specimens (Figs 4A-B, D-E, 7B, 8A); its distal process is distinctly triangular with a blunt, latero-distal angle, and its latero-distal margins are deeply embayed. Together with the left PM, this is the largest element of the plano-concave surface. The distal process and bilateral symmetry of the right LOP vary in larger specimens. Thus, in some individuals the right LOP becomes almost bilaterally symmetrical (Figs 4D-E, 7B, 8A), whereas in others left and right latero-distal margins of this plate differ in length and orientation with respect to the longitudinal body axis, so that its distal process is displaced with respect to this axis (Figs 4A,B, 11A).

The outline of plate A varies from subrectangular in small and medium specimens to elongate pentagonal or subtriangular in large individuals (Fig. 4A-E).

The PLM plates have 3-4 sharp, proximal lateral serrations with steep distal margins in small to medium specimens; in large specimens, the serrations are more numerous, blunt-ended and with less steep distal margins; size of the serrations does not seem to change at different ontogenetic stages (Figs 4A-E, 5C).

In the smallest individual (Fig. 4C,F), distal margins of the PM plates are much shorter than proximal margins, and the proximal excavation for insertion of the articulated appendage is shallower than in larger individuals.

Plates C20 and C22 are 2.5-3 times as long as wide and differ mainly in degree of curvature of their lateral margins and in length and orientation of their medio-distal margin. One isolated C20 (Fig. 8B) has a more elongate and concave medio-distal margin and broad median emargination in its proximal margin. In the same plate, a ridge runs for c. 2/3 plate width from the proximal end of its medio-distal margin to a thickened triangular area latero-distal to co-operculum; median 2/3 of ridge almost straight; lateral 1/3 bent strongly towards co-operculum. Shallow areas present just proximal to the ridge, and delimited proximally by a second, fainter transverse ridge running from median margin of C20 to a point c. 1/2 along maximum plate width before disappearing abruptly laterally.

***Adoketocarpus janeae* sp. nov.**
(Figs 11B,C, 12E, 13)

ETYMOLOGY. For Jane Jell, who helped collect the material described herein.

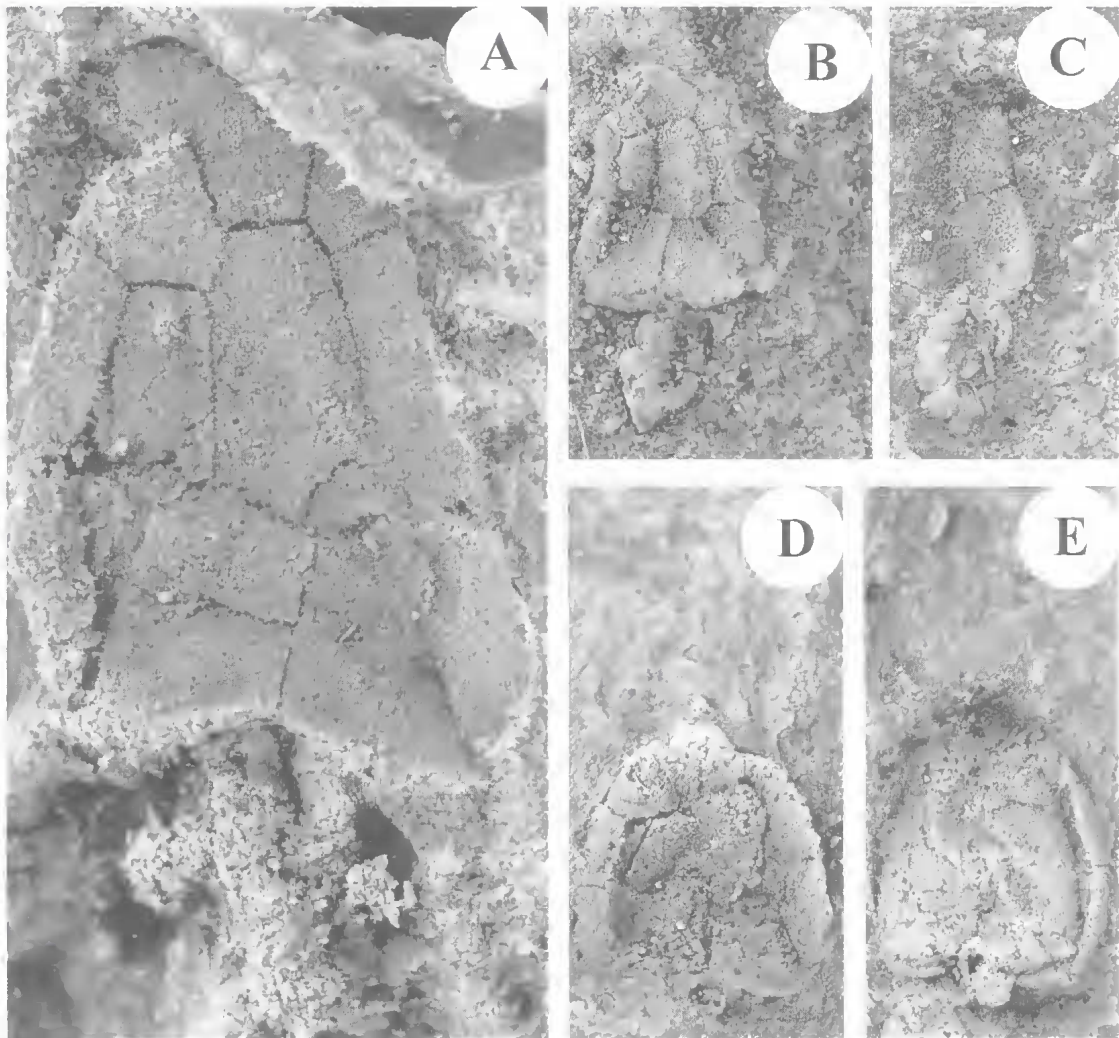


FIG. 11. A,D,E, *Adoketocarpus acheronticus* gen. et sp. nov., from NMVPL1927. A, plano-concave surface of QMF37208, $\times 9$. D,E, plano-concave and convex surfaces of QMF37214, $\times 12$. B,C, *Adoketocarpus janeae* gen. et sp. nov., from NMVPL252, plano-concave and convex surfaces of NMVP149391, $\times 12$.

MATERIAL. Holotype: NMVP100359. Paratype: NMVP100360 from NMVPL1924 on Mathieson's Creek north of Kinglake West (=T95 of Williams 1964); NMVP149391, 149392 from NMVPL252.

DIAGNOSIS. Lateral margins almost straight. Left DLM and right EXM/ILM subequal in length. Left LOP and right DLM smaller than other marginal plates and approximately equal in size. Left LOP median to left latero-distal angle of plano-concave surface. Plate A narrow and elongate. Plate C slightly wider proximally than distally.

DESCRIPTION. General aspect. Only those skeletal features which distinguish *A. janeae* from *A. acheronticus* are discussed in detail here.

Lateral margins of body straight for most of their length and only slightly converging distally. Left DLM and right EXM/ILM much longer than wide and of similar shape and size; distal margin of left DLM at 45° with longitudinal body axis. Free margins of left LOP (distal in position) and of right DLM gently convex; free margin of right DLM about 3 times as long as medio-proximal margin. Left LOP lying median to left latero-distal angle of plano-concave surface and contributing only to a small extent to left lateral

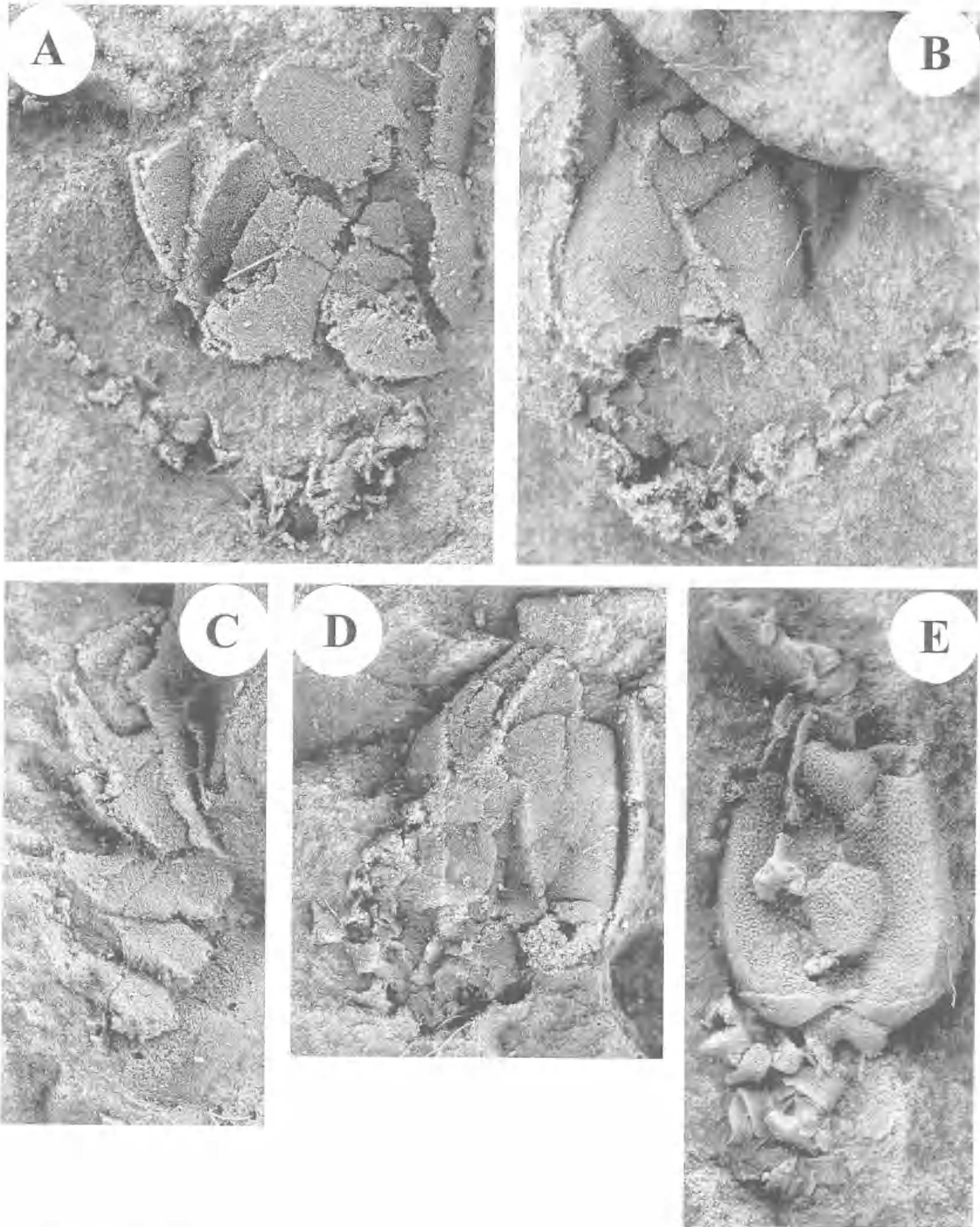


FIG. 12. A-D, *Adoketocarpus acheronticus* gen. et sp. nov., from NMVPL1927, $\times 10$. A,B, disrupted body and appendage QMF37202. C, isolated styloid and ossicles QMF37213. D, partial convex surface and ossicles QMF37212. E, *Adoketocarpus janeae* gen. et sp. nov., disrupted convex surface of NMVPL149392 from NMVPL252, $\times 10$.

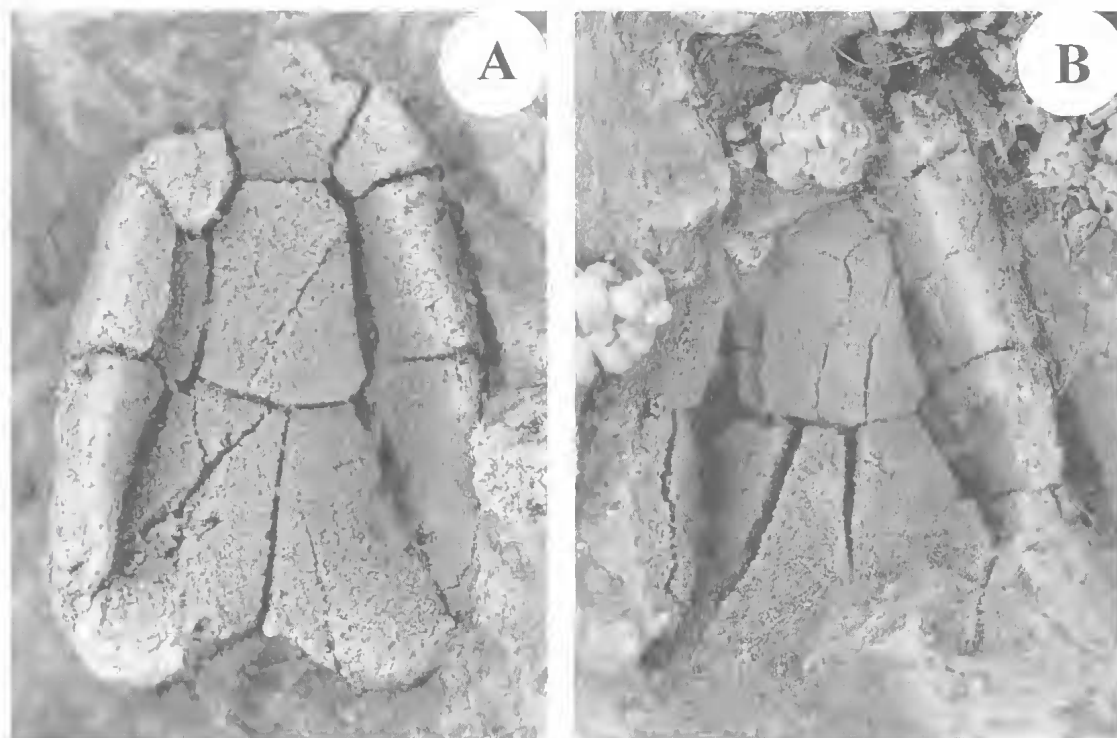


FIG. 13. *Adoketocarpus janeae* gen. et sp. nov., from NMVPL1924. A, NMVP100359, holotype, almost complete, slightly disrupted, plano-concave surface, $\times 10$. B, NMVP100360, partially disrupted, incomplete, plano-concave surface, $\times 10$.

body margin. Right LOP with semi-elliptical distal process and markedly sinuous proximo-lateral margins, and c. 1/2 as large as C; left latero-distal margin of right LOP at c. 120° with free margin of left LOP. Lateral 1/2 of proximal margin of each of the 2 PM plates passing gradually into median 1/2: the latter only slightly concave and meeting its antimere at c. 120° ; suture between left and right PM straight. C slightly wider proximally than distally. Suture between A and C gently concave leftward throughout most of its length. Plate A at least 3 times as long as wide and in contact with left arm of distal, chevron-shaped margin of left PM along very short suture. Robust, sharp serrations partly visible along disrupted lateral margin of right PLM in the less complete of the 2 specimens observed. Stereostructure of coarse pores and irregular, sinuous trabeculae; pores decreasing in size towards plate sutures.

Measurements. NMVP100359 (Fig. 13A) is 5.7mm wide and 7.8mm long.

REMARKS. Attribution of the Lower Devonian species to *Adoketocarpus* is based on the plating

pattern of the plano-concave surface, but only 4 individuals permit limited comparisons with the type species. The differences between the Lower Devonian and the Upper Silurian taxa warrant a distinct specific assignment for the former.

Such features of *A. janeae* as shape and relative proportions of left LOP and left DLM and high length/width ratio of A are similar to those in *E. savilli* Beisswenger, 1994 from the Llandeilo of Morocco (Fig. 3C). In *E. savilli* and *A. acheronticus*, the left LOP builds the left latero-distal angle of the plano-concave surface and the most proximal part of its lateral margin contributes to the left lateral body wall. In both species, the left latero-distal margin of the right LOP and the free margin of the left LOP meet at an obtuse angle. In *A. janeae*, the left LOP lies almost completely median to the left latero-distal angle of the plano-concave surface and its free margin is at c. 120° with the left latero-distal margin of the right LOP. *Adoketocarpus janeae* shows a more bilaterally symmetrical body outline than either *A. acheronticus* or *E. savilli* (Figs 3C,D, 13A), although elements of asymmetry are evident in the arrangement of the distal marginal

plates of the plano-concave surface and in the different length of the left and right lateral margins of the body.

The higher degree of bilateral symmetry of *A. janeae* is also observed in the shape of the right LOP, the distal process of which lies only slightly to the left of the longitudinal body axis. Because the only convex surface of *A. janeae* is not well preserved (Fig. 12E) its degree of asymmetry is uncertain.

COMPARISONS BETWEEN *ADOKETOCARPUS* AND OTHER PARANACYSTIDS

Members of the Paranacystidae Caster, 1954 (Ruta, 1997c) are readily identified by several features such as the plate configuration of the convex surface and the 2 unequal subcentral plates on the plano-concave surface. As defined by Caster (1954) the family includes *Paranacystis petrii* Caster, 1954, *P. simoneae* Ruta, 1997c, *Adoketocarpus acheronticus* and *A. janeae*. Haude (1995) placed *Yachalcystis triangularis* from the Lower Devonian of Argentina in the Paranacystidae, based on the 2 large, proximo-distally elongate plates on the convex surface and on details of the stereom. Ruta (1997c) tentatively assigned the Middle Devonian *Dalejocystis casteri* Prokop, 1963 from Bohemia to the Paranacystidae, based on its overall resemblance to *Y. triangularis*. However, both *Y. triangularis* and *D. casteri* are too poorly preserved for their affinities to be fully evaluated, and will not be considered further here. Because the material of *A. janeae* is incomplete, the following discussion focusses mainly on *A. acheronticus*, except where a direct comparison between the Lower Devonian form and other paranacystids is necessary.

The body outline is more asymmetrical in *A. acheronticus* than in either *Paranacystis* species. With the exception of the left and right PLM, the remaining lateral marginal plates of the plano-concave surface of *A. acheronticus* do not form pairs of elements of similar shape and size, and are smaller than either left or right PLM; conversely, in both *Paranacystis* species, the lateral marginal elements immediately distal to PLM are almost mirror images of each other and comparable in size with these plates. In *A. janeae*, the left DLM and the right EXM/ILM are similar in shape and size.

A. acheronticus differs from both *Paranacystis* species in that plate A is only slightly longer than

wide and much smaller than C; in addition, C is much wider in *A. acheronticus* than in either *Paranacystis* species; in *P. simoneae*, C has a robust, distal triangular process (Ruta, 1997c).

As in *P. simoneae*, the 2 PLM plates of *A. acheronticus* have a lateral longitudinal row of denticulations. In *P. simoneae*, these are smaller than in *A. acheronticus* and shaped like sub-elliptical, proximo-distally elongate knobs confined to the proximal 2/3 of left and right PLM. In both *Paranacystis* species, the proximal excavation for appendage insertion is wider and deeper than in *A. acheronticus*. The distal, subtrapezoidal plates of the convex surface are much larger with respect to C20 and C22 in *P. petrii* (convex surface not preserved in *P. simoneae*) than in *A. acheronticus*; in addition, the suture formed by the 2 subtrapezoidal plates is shorter in the latter than in *P. petrii*.

For Caster (1954), the distal plates of *P. petrii* were imbricate in life and acted as an ostial cover; he considered this feature diagnostic of the family. *A. acheronticus* suggests that ostial elements identified by Caster (1954; figs 1a-e, 2b) in *P. petrii* are homologous with the left LOP, right DLM and/or right LOP plates. In *A. acheronticus*, the right LOP is tightly sutured with the rest of the plano-concave surface and does not seem to have formed a flexible articulation in life. In a disrupted paratype of *P. petrii* (Caster, 1954, fig. 3b), the distal 1/2 of the internal mould of plano-concave surface shows a subpentagonal plate sutured on the right with a small trapezoidal element. These 2 plates correspond to the right LOP and right DLM of *A. acheronticus* respectively, based on shape and position (see Caster, 1954, fig. 1e). In *A. acheronticus* the distal margins of the left LOP and right DLM are partly visible when the convex surface is oriented towards the observer, suggesting that the so-called ostial elements of *P. petrii* are likely to be displaced and/or disrupted plates of the distal margin of the plano-concave surface.

Distal plate configuration of the plano-concave surface in *A. acheronticus* differs from that of *P. simoneae*, in which C carries a distal triangular process. The shape and position of this process resemble those of the right LOP in *A. acheronticus*; homology of this C process is uncertain. In *P. simoneae*, a small pit near the right proximal angle of the C process occupies the same relative position with respect to the body orifice as the subcircular depression on the underside of the right latero-distal angle of the right LOP of *A.*

acheronticus. However, the distal part of the plano-concave surface of *P. simoneae* is not well-known; Ruta (1997c) mentioned the possibility that some skeletal elements (possibly the left LOP and right DLM) in the only known specimen of this mitrate are either displaced or not preserved.

A. acheronticus permits a more accurate diagnosis of the Paranacystidae. The distal elements of the plano-concave surface did not act as an ostial cover, as surmised by Caster (1954) in *P. petrii*. Rather, this part of the skeleton was rigid and roofed over the body orifice. The distalmost region of the convex surface, on the other hand, was probably flexible, as indicated by the small, irregular plates surrounding the orifice platelets. This flexible integument is documented in several mitrates (Ubaghs, 1967, 1979; Jefferies & Lewis, 1978; Kolata & Jollie, 1982; Jefferies, 1986; Cripps, 1990; Parsley, 1991; Beisswenger, 1994; Ruta, 1997b).

DISCUSSION. In *A. acheronticus* the simplified plating pattern of the proximal 2/3 of the convex surface is probably a derived condition compared with that of the mitrocystitids and anomalocystitids. On the other hand, the pit on C20 is shared with several mitrocystitids (Chauvel, 1941; Ubaghs, 1961, 1967, 1979, 1994; Cripps, 1990; Ruta, 1997b) which are considered by many workers to be more primitive than the anomalocystitids (Jefferies, 1967, 1968, 1973, 1986, 1991; Craske & Jefferies, 1989; Cripps, 1990; Beisswenger, 1994; Ruta, 1997b, in press; Ruta & Theron, 1997; but see Ubaghs, 1979 and Parsley, 1991).

A twisted orifice at a high angle to the axis of the body is found in *Vizcainocarpus dentiger* (Ruta, 1997b), in young individuals of *Mitrocystites mitra* (Jefferies, 1968; Ubaghs, 1967) and in *Eumitrocystella savilli* (Beisswenger, 1994) among the mitrocystitids, although less pronounced asymmetry of this structure is observed in other mitrates (Thoral, 1935; Ubaghs, 1967, 1969, 1979; Jefferies, 1986).

There are fewer tightly sutured polygonal elements on the plano-concave surface of *A. acheronticus* than on other mitrocystitids or anomalocystitids. The 2 subcentral elements on the plano-concave surface also occur in *E. savilli* and most anomalocystitids, although this condition can be shown to have evolved in parallel in the 2 latter groups (Beisswenger, 1994; Ruta & Theron, 1997; Ruta, in press). In particular, the position of plate A, between C and the left lateral

marginal elements of the plano-concave surface, recalls the skeletal configuration of the allanicytidid anomalocystitids (Ruta & Theron, 1997).

The fewer plates of the convex surface and large C20 and C22 also occur in peltocystid mitrates (Thoral, 1935; Ubaghs, 1967, 1969; Jefferies, 1986; Parsley, 1991); however, these differ from *A. acheronticus* in several aspects of the plating pattern of the plano-concave surface. *A. acheronticus* and *E. savilli* have 2 subcentral, unequal plates on the plano-concave surface and a distal plate roofing over the orifice. In most mitrocystitids and all anomalocystitids, the orifice is delimited by a row of distal marginal plates on the plano-concave surface, consisting of a median (MOP) and two lateral (LOP) elements. Based on topological similarity, Beisswenger (1994) hypothesized that MOP (= plate n) was lost in *E. savilli*, and that the distalmost element of the plano-concave surface is an enlarged and medially displaced right LOP (= plate c of Beisswenger, 1994). This hypothesis was supported by three arguments, two of which also apply to *A. acheronticus*.

His first argument is based on the reconstructed internal features of the distalmost plate of the plano-concave surface of *E. savilli*, which '... carries the beginning of the oblique ridge and builds part of the lateral [body] wall as in other mitrates' (Beisswenger, 1994: 448). Part of the internal side of the plano-concave surface can be observed in *A. acheronticus* (Figs 7A-B, 8A) where the distal end of the oblique ridge is partly visible on the proximal 1/3 of the internal surface of right LOP. The right LOP is larger than the elements lying immediately proximal to it, shows the same spatial relationships with these as in *E. savilli* and closely resembles the like-named plate of the latter in its general shape and in the development of a blunt distal projection covering the orifice platelets. The right LOP of *A. acheronticus* does not contribute to the right lateral body wall to the same extent as its proposed homologue in *E. savilli*, in that it is slightly displaced to the left with respect to the main body axis, presumably as a result of increased torsion of the orifice caused by the loss of a left lateral marginal element.

In *A. acheronticus*, almost the complete course of the oblique ridge is visible on the convex surface as a result of compaction (Figs 4F, 6A, C-D, 7B, 9B), showing that the distalmost end of the ridge lies on the proximal part of the internal surface of the right LOP. On the plano-concave

surface, the suture between the right LOP and C (= plate 12 of Beisswenger, 1994) straddles the distalmost portion of the oblique ridge. The distalmost part of the ridge appears as an impression on the median half of the right distal subtrapezoidal plate of the convex surface.

The second of Beisswenger's (1994) arguments is an hypothesis of morphological transformation inferred from the first argument: loss of MOP and increase in size and leftward displacement of the right LOP would explain leftward twisting of the orifice. If correctly interpreted, this transformation is more evident in *A. acheronticus*, where the orifice opening forms an angle of about 30° with respect to the main body axis, than in *E. savilli*, where this angle is about 45°.

Beisswenger's (1994) third argument is not directly applicable to *A. acheronticus*, as it involves comparison between plate organization on the plano-concave surface of *E. savilli* (Fig. 3C) and *Mitrocystella incipiens* (Fig. 3B) which closely resemble each other in proportions and relative positions of the subcentral and of left and right lateral marginal plates. Comparing these similar arrangements to the more primitive arrangement in *M. harrandi* (Fig. 3A), major differences in the distal 1/3 of the plano-concave surface are interpreted as resulting from loss of plate B (= plate 11 of Beisswenger, 1994) in *E. savilli*. Plate configuration of the distal 1/3 of the plano-concave surface in *A. acheronticus* matches that of *E. savilli*, and suggests that B may be secondarily absent in the Australian taxon.

The number of lateral marginal plates in *A. acheronticus* is reduced by one on the right and on one the left with respect to *E. savilli*, and the relative size and spatial relationships of the elements lying to the left of C are very similar to those of the left LOP, left DLM and A plates (= plates b, 3 and 10 of Beisswenger (1994), respectively). Based on their shape and position, proximal left and right lateral marginal plates correspond to PLM (= plates l and f of Beisswenger (1994), respectively). Assuming the correct identification of the other plates, it is reasonable to hypothesize that the left ILM (= plate 2 of Beisswenger, 1994) was lost in *A. acheronticus*, and that such a loss brought A in contact with the left PLM and left PM.

The right lateral marginal plates are more difficult to interpret. Comparison with *E. savilli* indicates that a plate of the right side of the body was lost in *A. acheronticus*. This plate might

correspond to the right EXM or ILM (= plates 6 and 7 of Beisswenger (1994), respectively) in *E. savilli* (Ruta, in press), but it cannot be identified unambiguously; hence, our right EXM/ILM notation for the marginal plate lying to the right of C. Finally, the left and right PM correspond to plates i and h of Beisswenger (1994), respectively, based on their shape, position and internal surface.

The resemblance between *E. savilli* and *Adoketocarpus* has implications for the origin and diversification of the Paranacystidae. We propose that the Paranacystidae derive from an ancestor resembling *E. savilli* through a simplification of the plate configuration. Further steps in this lineage may have been the acquisition of bilateral symmetry and a greater elongation of the body. Compensation for the asymmetrical body outline may have been achieved through modification of the relative proportions of the marginal plates of the plano-concave surface. In *A. acheronticus*, plate asymmetries are evident on this surface, but in *A. janeae* and in other paranacystids (Caster, 1954; Ruta, 1997c), such asymmetries disappear or are drastically reduced. Bilateral symmetry probably occurred proximo-distally, affecting the marginal elements first (as in *A. janeae*) followed by the subcentral plates (as in *Paranacystis*).

CONCLUSIONS

Adoketocarpus: 1) is the first representative of the Paranacystidae Caster, 1954 recorded from Australia; 2) from the Upper Silurian predates the next earliest family record in the Lower Devonian of South America (Caster, 1954; Caster & Eaton, 1956; Haude, 1995); 3) provides great detail of its external and internal anatomy, throwing light on several poorly known aspects of the paranacystids and prompting re-interpretation of skeletal organization of the family (Caster, 1954; Haude, 1995; Ruta, 1997c); 4) provides additional evidence of the affinities between Siluro-Devonian mitrates from Australia and those from the Malvinokaffric Realm (Caster, 1954, 1956, 1983; Gill & Caster, 1960; Caster & Gill, 1967; Philip, 1981; Parsley, 1991; Haude, 1995; Ruta & Theron, 1997; Ruta, 1997c); 5) shows that the paranacystids probably evolved from the paraphyletic mitrocystitids; *E. savilli* closely resembles *Adoketocarpus*, especially in the plano-concave surface and in the strongly twisted orifice. Evolution of the paranacystids was characterized by progressive increase in the bilateral symmetry of the body and of the lateral marginal plates.

ACKNOWLEDGEMENTS

M.R. thanks the Queensland Museum and its staff for use of facilities and for hospitality, A.R. Milner (Birkbeck College, University of London) for comments and suggestions, B. Lefebvre (Université Claude Bernard, Lyon) and R.L. Parsley (Tulane University, New Orleans) for stimulating discussions and Julia Day and Simone Wells (Natural History Museum, London) for encouragement. R.P.S. Jefferies, A.C. Milner, S.J. Culver and L.R.M. Cocks (Natural History Museum, London) read the manuscript. P. Crabb (Natural History Museum, London) took most of the photographs. We thank Ron Parsley and Reimund Haude for their useful reviews but the views set out above are those of the authors alone. M.R. is in receipt of a European Community grant (Training and Mobility of Researchers). The Museum of Victoria is thanked for loan of the material and David Holloway and Fons Vandenberg are thanked for help with field collecting.

LITERATURE CITED

- BEISSWENGER, M. 1994. A calcichordate interpretation of the new mitrate *Eumitrocystella savilli* from the Ordovician of Morocco. *Paläontologische Zeitschrift* 68: 443-462.
- CASTER, K.E. 1952. Concerning *Enoploura* of the Upper Ordovician and its relation to other carpod Echinodermata. *Bulletins of American Paleontology* 34: 1-47.
1954. A new carpod echinoderm from the Paraná Devonian. *Anais da Academia Brasileira de Ciências* 26: 123-147.
1956. A Devonian placocystoid echinoderm from Paraná, Brazil. *Palaeontologia do Paraná (Centennial Volume)*: 137-148.
1983. A new Silurian carpod echinoderm from Tasmania and a revision of the Allanicystidiidae. *Alcheringa* 7: 321-335.
- CASTER, K.E. & EATON, T.H. Jr 1956. Microstructure of the plates in the carpod echinoderm *Paranacystis*. *Journal of Paleontology* 30: 611-614.
- CASTER, K.E. & GILL, E.D. 1967. Family Allanicystidiidae, new family. Pp. 561-564. In Moore, R.C. (ed.) *Treatise on invertebrate paleontology*. Part 5. Echinodermata 1. (Geological Society of America & University of Kansas: New York).
- CHAUVEL, J. 1941. Recherches sur les cystoïdes et les carpoïdes armoricains. *Mémoires de la Société Géologique et Minéralogique de Bretagne* 5: 1-286.
- CRASKE, A.J. & JEFFERIES, R.P.S. 1989. A new mitrate from the Upper Ordovician of Norway, and a new approach to subdividing a plesion. *Palaeontology* 32: 69-99.
- CRIPPS, A.P. 1990. A new stem craniate from the Ordovician of Morocco and the search for the sister group of the craniata. *Zoological Journal of the Linnean Society* 100: 27-71.
- GARRATT, M.J. 1983. Silurian and Devonian stratigraphy of the Melbourne Trough, Victoria. *Proceedings of the Royal Society of Victoria* 95:77-98.
- GILL, E.D. & CASTER, K.E. 1960. Carpod echinoderms from the Silurian and Devonian of Australia. *Bulletins of American Paleontology* 41: 5-71.
- HAUDE, R. 1995. Echinodermen aus dem Unter-Devon der argentinischen Präkordillere. *Neues Jahrbuch für Geologie und Paläontologie, Abhandlungen* 197: 37-86.
- JAEKEL, O. 1918. Phylogenie und System der Pelmatozoen. *Paläontologische Zeitschrift* 3: 1-128.
- JEFFERIES, R.P.S. 1967. Some fossil chordates with echinoderm affinities. Pp. 163-208. In Millot, N. (ed.) *Echinoderm Biology*. (Academic Press: London).
1968. The Subphylum Calcichordata (Jefferies 1967) – primitive fossil chordates with echinoderm affinities. *Bulletin of the British Museum (Natural History), Geology Series* 16: 243-339.
1973. The Ordovician fossil *Lagynocystis pyramidalis* (Barrande) and the ancestry of *Amphioxus*. *Philosophical Transactions of the Royal Society of London, Series B* 265: 409-469.
1986. The ancestry of the vertebrates. (British Museum (Natural History): London).
1991. Two types of bilateral symmetry in the Metazoa: chordate and bilaterian. Pp. 94-127. In Bock, G. R. & Marsh, J. (eds) *Biological asymmetry and handedness*. (John Wiley & Sons: Chichester).
- JEFFERIES, R.P.S. & LEWIS, D.N. 1978. The English Silurian fossil *Placocystites forbesianus* and the ancestry of the vertebrates. *Philosophical Transactions of the Royal Society of London, Series B* 282: 205-323.
- KOLATA, D.R., FREST, T.J. & MAPES, R.H. 1991. The youngest carpod: occurrence, affinities and life mode of a Pennsylvanian (Morrowan) mitrate from Oklahoma. *Journal of Paleontology* 65: 844-855.
- KOLATA, D.R. & JOLLIE, M. 1982. Anomalocystitid mitrates (Stylophora, Echinodermata) from the Champlainian (Middle Ordovician) Guttenberg Formation of the Upper Mississippi Valley Region. *Journal of Paleontology* 56: 531-565.
- PARSLEY, R.L. 1991. Review of selected North American mitrate stylophorans (Homalozoa: Echinodermata). *Bulletins of American Paleontology* 100: 5-57.
- PHILIP, G.M. 1981. *Notocarpus garratti* gen. et sp. nov., a new Silurian mitrate carpod from Victoria. *Alcheringa* 5: 29-38.

- RUTA, M. 1997a. Redescription of the Australian mitrate *Victoriacystis* with comments on its functional morphology. *Alcheringa* 21: 81-101.
- 1997b. A new mitrate from the lower Ordovician of southern France. *Palaeontology* 40: 363-383.
- 1997c. First record of a paranacystid mitrate from the Bokkeveld Group of South Africa. *Palaeontologia Africana* 34: 15-25.
- In press. A cladistic analysis of the anomalocystitid mitrates. *The Zoological Journal of the Linnean Society*.
- RUTA, M. & JELL, P.A. 1999. Two new anomalocystitid mitrates from the Lower Devonian Humevale Formation of central Victoria. *Memoirs of the Queensland Museum* 43: 399-422.
- RUTA, M. & THERON, J.N. 1997. Two Devonian mitrates from South Africa. *Palaeontology* 40: 201-243.
- TALENT, J.A. 1967. Silurian sedimentary petrology and palaeontology. *Bulletin of the Geological Survey of Victoria* 59: 24-29.
- THORAL, M. 1935. Contribution à l'étude paléontologique de l'Ordovicien inférieur de la Montagne Noire et révision sommaire de la faune cambrienne de la Montagne Noire. (Imprimerie de la Charité: Montpellier). 363p.
- UBAGHS, G. 1961. Un échinoderme nouveau de la classe des Carpoïdes dans l'Ordovicien inférieur du département de l'Herault (France). *Compte Rendu Hebdomadaire des Séances de l'Académie des Sciences, Paris* 253: 2565-2567.
1967. Stylophora. Pp. 496-565. In Moore, R.C. (ed.) *Treatise on invertebrate paleontology. Part 5. Echinodermata 1(2)*. (Geological Society of America & University of Kansas: New York).
1969. Les échinodermes carpoïdes de l'Ordovicien inférieur de la Montagne Noire (France). *Cahiers de Paléontologie*. (éditions du Centre National de la Recherche Scientifique: Paris). 112p.
1979. Trois Mitrata (Echinodermata, Stylophora) nouveaux de l'Ordovicien de Tchécoslovaquie. *Paläontologische Zeitschrift* 53: 98-119.
1994. Échinodermes nouveaux (Stylophora, Eocrinoidea) de l'Ordovicien inférieur de la Montagne Noire (France). *Annales de Paléontologie. Invertébrés* 80: 107-141.
- VANDENBERG, A.H.M. 1988. Silurian-Middle Devonian. Pp. 103-146. In Douglas, J.G. & Ferguson, J.A. (eds) *Geology of Victoria*. (Victorian Division of the Geological Society of Australia: Melbourne).
1992. Kilmore 1:50,000 map and geological report. *Geological Survey of Victoria Report* 91: 1-86, + map.
- WILLIAMS, G.E. 1964. The geology of the Kinglake District, central Victoria. *Proceedings of the Royal Society of Victoria* 77: 273-328.
- WITHERS, R.B. 1933. A new genus of fossil king crabs. *Proceedings of the Royal Society of Victoria* 45: 18-22.